HHS Public Access

Author manuscript

Neurobiol Dis. Author manuscript; available in PMC 2017 May 01.

Published in final edited form as:

Neurobiol Dis. 2016 May ; 89: 10–22. doi:10.1016/j.nbd.2016.01.017.

STAT3 and SOCS3 regulate NG2 cell proliferation and differentiation after contusive spinal cord injury

Amber R. Hackett[1,*], **Do-Hun Lee**[1,*], **Abdul Dawood**[1], **Mario Rodriguez**[1], **Lucy Funk**[1], **Pantelis Tsoulfas**[1], and **Jae K. Lee**[1]

[1]Miami Project to Cure Paralysis, Department of Neurological Surgery, University of Miami School of Medicine, Miami, FL 33136

Abstract

NG2 cells, also known as oligodendrocyte progenitors or polydendrocytes, are a major component of the glial scar that forms after spinal cord injury. NG2 cells react to injury by proliferating around the lesion site and differentiating into oligodendrocytes and astrocytes, but the molecular mechanism is poorly understood. In this study, we tested the role of the transcription factor STAT3, and its suppressor SOCS3, in NG2 cell proliferation and differentiation after spinal cord injury. Using knockout mice in which STAT3 or SOCS3 are genetically deleted specifically in NG2 cells, we found that deletion of STAT3 led to a reduction in oligodendrogenesis, while deletion of SOCS3 led to enhanced proliferation of NG2 cells within the glial scar after spinal cord injury. Additionally, STAT3 and SOCS3 were not required for astrogliogenesis from NG2 cells after spinal cord injury. Interestingly, genetic deletion of STAT3 and SOCS3 did not have opposing effects, suggesting that SOCS3 may have targets other than STAT3 pathway in NG2 cells after spinal cord injury. Altogether, our data show that both STAT3 and SOCS3 play important, yet unexpected, roles in NG2 cell proliferation and differentiation after spinal cord injury.

Graphical Abstract

Corresponding author: Jae K. Lee, PhD, Miami Project to Cure Paralysis, Department of Neurological Surgery, University of Miami School of Medicine, 1095 NW 14th Terrace, LPLC 4-19, Miami, FL 33136, JLee22@med.miami.edu.

*These authors contributed equally to this work

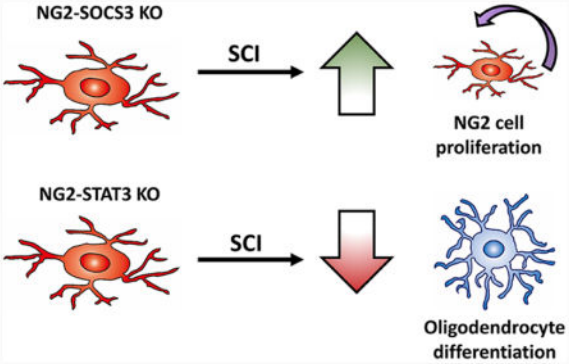

Keywords

Oligodendrocyte progenitor cells; astrocytes; glial scar; oligodendrocytes

Introduction

Oligodendrocyte progenitor cells (OPCs), also known as NG2 cells, are capable of differentiating into oligodendrocytes in the developing and the adult CNS (Nishiyama et al., 2009) and comprise approximately 70% of all dividing cells in the adult spinal cord (Horner et al., 2000). Although most studies focus on the role of NG2 cells in remyelination after spinal cord injury (SCI), less is known about their contribution to the glial scar (Levine, 2015, Son, 2015). Several studies implicate their production of chondroitin sulfate proteoglycans (CSPGs) (Dou and Levine, 1994, Levine, 1994, Petrosyan et al., 2013, Tan et al., 2006) and capacity to form synapses with dystrophic axons (Filous et al., 2014) to be largely inhibitory for axon regeneration. In addition, NG2 cells react to injury in a similar manner to reactive astrocytes in that they become hypertrophic and proliferate in the penumbra surrounding the injury site (McTigue et al., 2001, Zai and Wrathall, 2005). In fact, NG2 cells have been shown to differentiate into $GFAP^+$ astrocytes after several models of CNS injury (Komitova et al., 2011, Sellers et al., 2009, Tripathi et al., 2010, Zawadzka et al., 2010). However, the signaling pathways involved in the proliferation and differentiation of NG2 cells after SCI are not well understood.

Cytokines such as CNTF and LIF have been suggested to be important for NG2 cell proliferation and differentiation into oligodendrocytes and astrocytes *in vitro* as well as development of oligodendrocytes *in vivo* (Barres et al., 1996, Ishibashi et al., 2009, Mayer et al., 1994). The best characterized signaling pathway for many of these cytokines is activation of the JAK-STAT3 pathway through the gp130 receptor. This pathway is negatively regulated by SOCS3, which binds to the gp130-JAK complex. Cytokine expression is increased in the glial scar region after contusive SCI (Tripathi and McTigue, 2008, Zai et al., 2005) and high levels of phospho-STAT3, which is nearly undetectable in the uninjured spinal cord, are found in NG2 cells in this region (Hesp et al., 2015, Tripathi and McTigue, 2008). The JAK/STAT3 signaling pathway has also been implicated in astrocyte differentiation from $Nestin^+$ cortical precursor cells due to the binding of STAT3 to the GFAP promoter (Bonni et al., 1997, Nakashima et al., 1999b), and astrogliogenesis

and oligodendrogenesis is impaired in LIF KO mice and gp130 KO mice (Bugga et al., 1998, Nakashima et al., 1999a). Furthermore, both STAT3 and SOCS3 have been implicated in astroglial scar formation after SCI (Herrmann et al., 2008, Okada et al., 2006, Wanner et al., 2013), but their role in NG2 cells after SCI is not known.

We hypothesized that STAT3 is necessary for NG2 cell proliferation and differentiation after contusive SCI. We tested this hypothesis *in vivo* after SCI using genetic deletion of STAT3 or its suppressor SOCS3 specifically in NG2 cells. Our data indicate that after SCI, SOCS3 is an important regulator of NG2 cell proliferation, while STAT3 is important for oligodendrogenesis. Additionally, we determined that STAT3 and SOCS3 were dispensable for astrogliogenesis from NG2 cells after contusive SCI. Interestingly, genetic deletion of STAT3 and SOCS3 did not have opposing effects, revealing an unexpected molecular mechanism of NG2 cell proliferation and differentiation after SCI.

Materials and Methods

Animals

NG2-CreER mice, obtained from The Jackson Laboratory (stock 008538 (Zhu et al., 2011)), were bred to Rosa26-tdTomato reporter mice (kindly donated by Dr. Fan Wang, Duke University, Durham, NC. (Arenkiel et al., 2011)) to produce NG2-CreER^{+}/Rosa26-tdTomato$^{F/+}$ offspring, referred to as NG2-tdTomato or WT mice. To generate NG2 cell-specific deletion of STAT3, NG2-tdTomato mice were bred to STAT3 floxed mice, obtained from The Jackson Laboratory (stock 016923 (Moh et al., 2007)), to produce NG2-CreER^{+}/Rosa26-tdTomato$^{F/+}$/STAT3$^{F/F}$ mice, referred to as NG2-STAT3 KO mice. To generate NG2 cell-specific deletion of SOCS3, NG2-tdTomato mice were bred to SOCS3 floxed mice, obtained from The Jackson Laboratory (stock 010944 (Mori et al., 2004)), to produce NG2-CreER^{+}/Rosa26-tdTomato$^{F/+}$/SOCS3$^{F/F}$ mice, referred to as NG2-SOCS3 KO mice. Since the only commercially available antibodies against RFP were produced in a rabbit, and tdTomato fluorescence was destroyed by our antigen retrieval technique, we generated NG2-EYFP mice (NG2-CreER bred to Rosa26-EYFP from The Jackson Laboratory (stock 006148, (Srinivas et al., 2001)) in which a chicken GFP antibody can be used with rabbit antibodies that we could not use for colabeling studies in NG2-tdTomato tissue. All mice were of pure C57BL/6 genetic background. All procedures involving animals were approved by the University of Miami Institutional Animal Care and Use Committee and followed NIH guidelines.

Surgery

Six to 8 week old female mice were injected i.p. (intraperitoneal) with 0.124mg/g body weight of tamoxifen (MP Biomedicals) as previously described (Lee et al., 2009) for 5 consecutive days. One week after the last injection, mice were anesthetized (ketamine/xylazine, 100 mg/15 mg/kg i.p.) and received contusive SCI as previously described (Lee and Lee, 2013, Zhu et al., 2015). Mice received a T8 laminectomy, and the spinal column stabilized using spinal clamps, and then received a moderate (75 kDyne) SCI using an Infinite Horizons impactor device (Precision Systems and Instrumentation, LLC). Mice received post-operative treatment of antibiotics (Baytril, 10 mg/kg), and analgesics

(buprenorphine, 0.05 mg/kg) diluted into 1 mL of Lactated Ringer's solution injected subcutaneously twice per day for the first week following surgery. Mice received manual bladder expression twice daily until the end of the experiment.

Histology

Mice were anesthetized and then transcardially perfused with 4% paraformaldehyde in phosphate buffered saline (PBS). Spinal cords were dissected and postfixed in 4% paraformaldehyde in PBS for 2 hours, and cryoprotected in 30% sucrose in PBS overnight. 8 mm segments of the spinal cord centered at the injury site were embedded in OCT compound (Tissue-Tek) and sagittal serial sections (16 μm) were cut using a cryostat. Sections were immunostained by incubating in primary antibodies in 5% Normal Goat Serum in PBS with 0.3% Triton-X overnight at 4°C. Primary antibodies used were: RFP (Rockland 600-401-379S, 1:1000), GFAP (Invitrogen 130300, 1:1000 or Dako Z033429, 1:1000), APC/CC1 (Millipore OP80 Ab-7, 1:500), NG2 (Millipore AB5320, 1:200), GFP (Abcam ab13970, 1:2000), PDGFRβ (Abcam ab32570, 1:200), Iba1 (Wako 019-19741, 1:500), Olig2 (Millipore AB9610, 1:200), and phospho-STAT3 Y705 (Cell Signaling 9145S, 1:100). Following primary antibody incubation, sections were washed and incubated in species-appropriate Alexa Fluor IgG (H+L) secondary antibodies (Invitrogen, 1:500) at room temperature for 1 hour. For CC1, goat-anti-mouse IgGγ2b secondary antibody was used (Invitrogen A-21141, 1:500). Slides were mounted using Vectashield with DAPI (Vector Laboratories H-1200). Images were obtained using a Nikon Eclipse Ti fluorescent microscope or an Olympus FluoView 1000 confocal microscope. For phospho-STAT3 staining, we performed antigen retrieval by incubating slides in L.A.B. solution (Polysciences, Inc.) for 15 minutes at 60°C prior to immunostaining.

EdU Proliferation Assay

Mice were injected i.p. with 50 mg/kg of EdU (Invitrogen A10044) in 2% DMSO in PBS at 2, 3, and 4 days after SCI and sacrificed at 7 days after SCI. Tissues were prepared for histology as described above, and EdU was detected by using Click-iT EdU Alexa Fluor 488 Imaging Kit (Invitrogen C10337) according to manufacturer's instructions. Sections were subsequently immunostained as described above. All sections were counterstained with DAPI, and only EdU^+ cells that were also $DAPI^+$ were included in the quantification.

TUNEL Apoptosis detection

Terminal deoxynucleotidyl transferase dUTP nick end labeling (TUNEL) staining was performed as described previously (Gavrieli et al., 1992) with some modifications. Frozen sections were permeabilized in 2 parts ethanol, 1 part acetic acid for 5 minutes at −20 °C, then washed thoroughly with PBS. Sections were incubated in PBS at 37 °C for 30 minutes then incubated with 40 μg/mL proteinase K in PBS for 15 minutes at 37 °C. Digestion was stopped by washing with PBS and then slides were pretreated with TdT Buffer (25mM Tris-HCl, 200 mM Sodium Cacodylate, 0.25 mg/ml BSA, 1mM Cobalt Chloride, Roche) at 37°C for 10 minutes. To perform end-labeling, TdT Buffer was combined with terminal transferase (Roche, 400 U/slide) and Biotin-16-dUTP (Roche, 4 μM) and added to slides for 1 hour at 37 °C. Slides were thoroughly washed with PBS then blocked for 30 minutes with 5% Normal Goat Serum in PBS with 0.3% Triton-X, then incubated with Alexa-Fluor

conjugated streptavidin (Invitrogen, 1:500) for 30 minutes at 37 °C. Slides were subsequently immunostained as described above. All sections were counterstained with DAPI, and only TUNEL$^+$ cells that were also DAPI$^+$ were included in the quantification.

Histology Quantification

For histological quantifications, three consecutive sagittal spinal cord sections (per animal) centered on the injury epicenter and spaced 160 μm apart were imaged on Nikon Eclipse Ti fluorescent microscope. Using NIS Elements AR Software, a contour was drawn around the GFAP-negative area (lesion site) and used as a reference point to delineate 250 μm intervals rostral and caudal from the lesion site (thus all sections were co-stained with GFAP). The area for each interval was determined using NIS Elements AR Software. Regions 0–250 μm and 250–500 μm were considered as within the glial scar whereas the 1000–1250μm area was considered outside the glial scar based on the hypertrophic and interweaving GFAP processes that reactive astrocyte typically display. For these quantifications, all tdTomato$^+$ cells on each section were counted, excluding those with obvious tubular pericyte morphology (as shown in Fig. 2F–I, 2T–Y), and the percentage that colocalized with each antigen was calculated. Only tdTomato$^+$ cells that were also DAPI$^+$ were included in the analysis. The percentages were determined for all three sections and then averaged per animal. For uninjured samples, the same analysis was used except that the contours were drawn from the center of the section and the values for the intervals were averaged. For oligodendrocyte quantifications, only cells with round bright CC1 staining restricted to the cell soma were counted. We confirmed in separate staining that virtually all cells that conformed to these characteristics were also olig2$^+$ (Supplementary Fig. 3). Additionally, since all sections were stained with GFAP to delineate the glial scar, we took care to ensure that CC1$^+$ cells included in the analysis were not also GFAP$^+$, as previously reported after rat contusive SCI (McTigue et al., 2001).

For GFAP quantification, we used unbiased stereological principles using the Stereoinvestigator software. Contours were drawn around the GFAP-negative area and a line tool was used to delineate 1250 μm rostral and caudal to the lesion site. Using the Optical Fractionator Workflow, random 150 by 250 μm counting fields were sampled from this delineated region and counted at 63x magnification. Data from these counts were imported into Neuroexplorer software and the number of tdTomato$^+$GFAP$^+$ cells was determined within each 250 μm interval. For uninjured sections, the contours were drawn in the same regions starting from the center of the section. Five sagittal spinal cord sections were analyzed per animal and the numbers from these sections were summed.

NG2 cell isolation and culture

NG2 cells were isolated and cultured as previously described (Dincman et al., 2012) with some modifications. Postnatal day 5–7 mouse brains from either Rosa26-tdTomato$^{F/+}$ mice, Rosa26-tdTomato$^{F/+}$/STAT3$^{F/F}$ mice, or Rosa26-tdTomato$^{F/+}$/SOCS3$^{F/F}$ mice were manually dissociated into a single cell suspension using a papain based kit (Miltenyi Biotec) according to manufacturer's instructions. Dissociated cells were blocked with FcR and incubated with PDGFRα microbeads (Miltenyi Biotec), and then separated using LS columns (Miltenyi Biotec) on Midi MACS separators (Miltenyi Biotec) according to

manufacturer's instructions. Cells were plated at 50,000 cell/cm^2 onto 0.1 mg/mL Poly-D-Lysine (Millipore) coated plates and expanded in OPC media (DMEM/F-12 (Gibco) supplemented with 2% B27 (Gibco), 1% N2 (Gibco), 1% Antibiotic-antimycotic (Gibco), 40 ng/mL bFGF (Sigma), and 20 ng/μL PDGF-AA (Gibco)). Cells were determined to be around 95 % pure using staining against PDGFRα (BD Biosciences 558774, 1:500).

Lentiviral production and administration

LV-Cre plasmid, a gift from Dr. Inder Verma (Addgene plasmid # 12106) (Pfeifer et al., 2001), was amplified using Gen Elute Endotoxin-Free Maxiprep (Sigma) and verified by sequencing. Lentivirus was prepared by the University of Miami Viral Vector Core (titer of 5.5 x 10^7 pg/mL). Lentivirus was diluted at 1:1000 in OPC media and removed from the cells by a full media change after 24 hours. This dilution resulted in a recombination efficiency of about 50%, as determined by expression of the tdTomato in the cultured cells. Deletion of STAT3 and SOCS3 were confirmed by Western blot analysis using total lysate from each well.

Western blot

Cold lysis buffer (20 mM Tris-HCl pH 7.5, 50 mM NaCl, 0.5% TritonX-100, 0.25% Deoxycholate, 1% SDS, 5 mM NaF, 1 mM EDTA pH 8.0, 1 mM PMSF, protease inhibitors (Roche) and phosphatase inhibitor cocktail (Sigma) were added to cells and homogenized by passing through a 30 gauge needle 5 times. Protein concentrations were determined by using the Pierce BCA assay (Thermo Scientific). 10 μg of protein was boiled for 10 minutes in NuPAGE LDS Sample Buffer (Invitrogen) and separated with SDS-PAGE using a 10% acrylamide gel, and then transferred to a PVDF membrane. Membranes were washed and then blocked in 5% BSA in TBST at room temperature for 1 hour followed by incubation in primary antibodies overnight at 4°C. The next day, membranes were washed and then incubated in species appropriate HRP-conjugated secondary antibody (Cell Signaling 1:10,000) for 1 hour at room temperature. After washing, membranes were incubated in Supersignal West Pico (Thermo Scientific) chemiluminescence solution for 5 min and then exposed to film (Phoenix Research Products). Primary antibodies were: phospho-STAT3 Y705 (Cell Signaling 9145S,1:2000), total STAT3 (Cell Signaling 4904S, 1:1000), SOCS3 (Abcam ab16030, 1:1000), and β-actin (Sigma A2228-100UL, 1:10,000). Two separate biological experiments were performed for each analysis.

Statistics

GraphPad Prism software was used to perform statistical analyses. Either One-Way ANOVA or Two-Way ANOVA with repeated measures and Tukey's or Bonferroni's *post hoc* test were used, where $p<0.05$ was considered significant. All error bars are SEM.

Results

Distribution of NG2 lineage cells after contusive SCI

First, we investigated the distribution of NG2 derived cells in wild type mice after SCI using genetic fate-mapping strategies. We generated NG2-tdTomato mice (NG2-CreER mice bred to Rosa26-tdTomato reporter mice, referred to as WT mice hereafter) in which upon

tamoxifen injection, a population of NG2 cells become permanently labeled with tdTomato as they proliferate and differentiate. One week after tamoxifen injections, mice received a mid-thoracic contusive SCI, and were sacrificed at either 1 or 4 weeks after injury (Fig. 1A). After SCI, we analyzed 3 different regions determined by their distance from the GFAP$^-$ lesion border. 0–250 μm and 250–500 μm were considered to be within the glial scar region while 1000–1250 μm was considered outside the glial scar based on the morphology of the GFAP$^+$ cells (see Methods). At 1 and 4 weeks after SCI (Fig. 1B, F–K), the density of tdTomato$^+$ NG2 lineage cells significantly increased in both regions of the glial scar, while the density outside of the glial scar remained similar to uninjured controls (pericytes, macrophages and fibroblasts were excluded from the analysis, as explained below). The density of tdTomato$^+$ NG2 lineage cells did not significantly change from 1 to 4 weeks after SCI. In the uninjured spinal cord, we observed an even distribution of tdTomato$^+$ cells throughout the spinal cord (Fig. 1B, C–E), which did not significantly change in number between the corresponding 1 and 4 weeks. Thus, NG2 lineage cell density increases within the glial scar region by one week after SCI and is maintained for at least 4 weeks.

To determine the recombination efficiency of the NG2-CreER mouse line, we bred it to the Rosa26-EYFP reporter mice as this allowed us to co-stain with the rabbit NG2 antibody (see methods). At 1 day after the last tamoxifen injection, over 95% of EYFP cells colocalized with NG2 (data not shown). We observed that 30% of total NG2$^+$ glia were EYFP$^+$ (Fig 2A). In addition to NG2$^+$ glia (Fig. 2B–E), NG2$^+$ pericytes (Fig. 2F–I) were also labeled, but were morphologically distinct from NG2 glia. One week after SCI, we stained for NG2 and saw that approximately 40–60% of EYFP$^+$ cells (using the NG2-EYFP mice) still expressed NG2 in the glial scar region (0–500μm) (Fig. 2J–P). We excluded non-NG2 lineage cells, such as pericytes, macrophages and fibroblasts, which may also express the NG2 antigen before and/or after SCI. We excluded NG2$^+$ pericytes based on their tubular morphology around blood vessels with a hollow circular shape, a crescent moon shaped nucleus (Fig. 2W–Y), and small cell soma size (Fig. 2F–I) compared to NG2$^+$ glia, which have larger cell soma and a highly branched morphology (Fig. 2B–E). Fibroblasts that contribute to the fibrotic scar after SCI (Goritz et al., 2011, Soderblom et al., 2013) were identified as being PDGFRβ$^+$ cells, which were located predominantly in the GFAP$^-$ area whereas EYFP$^+$ cells were present surrounding this region (Fig. 2Q–Y). With occasional exceptions (Fig. 2T–V, yellow arrows), PDGFRβ$^+$ YFP$^+$ cells were not present in the glial scar region. Although previous studies have reported upregulation of NG2 in macrophages after injury (Bu et al., 2001, McTigue et al., 2006), we did not observe any Iba1$^+$EYFP$^+$ cells, most likely due to the fact that our genetic lineage tracing strategy only labels cells that express NG2 during the pre-SCI tamoxifen administration period (Fig. 2Z–AC). Taken together, our data suggest that the fluorescently labeled (tdTomato or EYFP) cells in our quantifications were predominantly NG2$^+$ glia and their progeny.

SOCS3 deletion increases NG2 lineage cell density within the glial scar after SCI

Previous studies have shown that CNTF, a ligand for the STAT3 pathway, expression is increased in the glial scar region after contusive SCI and phospho-STAT3 is expressed in NG2 cells after SCI (Tripathi and McTigue, 2008, Zai et al., 2005). Thus, we hypothesized that STAT3 may play an important role in the proliferation and/or differentiation of NG2

cells after SCI. We found that in the uninjured spinal cord, there were very few cells expressing phospho-STAT3 (Fig. 3A–B). However, 2 weeks after SCI, a large number of NG2 lineage cells adjacent to the lesion expressed phospho-STAT3 (Fig. 3C–H). To test the role of STAT3 and its suppressor SOCS3, we bred NG2-CreER mice to STAT3 and SOCS3 floxed mice as well as Rosa26-tdTomato reporter mice to generate compound mutants in which injection of tamoxifen induces deletion of STAT3 or SOCS3 as well as expression of tdTomato in the same cell (mice will be referred to as WT, NG2-STAT3 KO and NG2-SOCS3 KO mice). We were unable to confirm STAT3 and SOCS3 deletion in our tissue sections due to antibody limitations; none of the commercially available SOCS3 antibodies we tested were compatible with immunohistochemistry, and the antigen retrieval step required for phospho-STAT3 antibody was not compatible with RFP immunostaining. Thus, we confirmed STAT3 and SOCS3 deletion using primary NG2 cells from the same STAT3 and SOCS3 floxed mouse lines that we used for our SCI experiments. Upon transduction with lentivirus expressing Cre recombinase (LV-Cre), approximately 50% of the cultured cells expressed tdTomato (i.e. recombination efficiency) (Fig. 4A–C). Accordingly, there was about a 50% decrease in STAT3 and SOCS3 protein level in the total cell homogenate as determined by Western blot analysis (Fig. 4A, D–F). Additionally, treatment with CNTF led to increased levels of phospho-STAT3 in WT and an even greater increase in SOCS3 KO NG2 cells (Fig. 4G–H). In addition, the floxed STAT3 and SOCS3 mouse lines are well-characterized in the literature using many different cell-specific Cre driver mice including astrocytes and macrophages (Herrmann et al., 2008, Okada et al., 2006, Qin et al., 2012). Taken together, our data confirm the deletion of STAT3 or SOCS3 in NG2 cells.

Next, we sought to test the role of STAT3 and SOCS3 in NG2 lineage cell proliferation. In the uninjured spinal cord, WT, NG2-STAT3 KO, and NG2-SOCS3 KO mice showed a similar density of $tdTomato^+$ cells that were evenly distributed throughout the spinal cord (Fig. 5A, D, G, J). At 1 week after SCI (Fig. 5B, E, H, K), the density of $tdTomato^+$ cells was higher in the glial scar region in NG2-SOCS3 KO mice as compared to WT controls, while the density in NG2-STAT3 KO mice was not significantly different from WT controls. Similar trends were observed at 4 weeks after SCI (Fig. 5C, F, I, L). Taken together, our data indicate that SOCS3 is important for regulating the number of NG2 lineage cells present in the glial scar, but STAT3 is dispensable in this process.

Next, we determined whether the increased number of cells present after SOCS3 deletion was due to enhanced proliferation and/or survival. To determine the effect of SOCS3 deletion on NG2 cell proliferation we injected EdU on days 2–4 after SCI in WT and NG2-SOCS3 KO mice. (Fig. 6A). We chose this time interval because previous studies determined around 3 days after SCI to be the peak of NG2 cell proliferation (Lytle and Wrathall, 2007). We observed that the density as well as the percent of $EdU^+tdTomato^+$ cells (Fig. 6R–S) was increased in NG2-SOCS3 KO mice (Fig. 6L–Q) compared to WT (Fig. 6F–K) in the glial scar region, but was similar in distal regions. To determine the effect of SOCS3 deletion on NG2 cell survival, we used TUNEL staining to label apoptotic cells at 1 week after SCI (Fig. 7). The majority of $TUNEL^+$ cells were within the lesion and in surrounding regions as previously reported (Liu et al., 1997). A small proportion of these $TUNEL^+$ cells colocalized with tdTomato (Fig. 7G–L). Compared to wildtype mice (Fig. 7A–C), NG2-SOCS3 KO mice (Fig. 7D–F) displayed a trend toward a lower percentage of

TUNEL$^+$ tdTomato$^+$ cells in the glial scar region, but this difference was not statistically significant (Fig. 7M). Only DAPI$^+$ cells were included in our analysis (Fig. 7K, L). Proliferation and survival assays were not performed in NG2-STAT3 KO mice since they did not show changes in cell density at any of the time points tested. Taken together, our data suggest that the increased numbers of NG2 lineage cells after SOCS3 deletion is mostly due to cell proliferation.

STAT3 deletion in NG2 cells reduces oligodendrogenesis but not astrogliogenesis after SCI

To determine the role of STAT3/SOCS3 on NG2 cell differentiation into oligodendrocytes, we quantified the percentage of tdTomato$^+$ cells that colocalized with the mature oligodendrocyte marker CC1 in WT (Fig. 8A–F, S–T), NG2-STAT3 KO (Fig. 8M–T), and NG2-SOCS3 KO mice (Fig. 8G–L, S–T). CC1$^+$ cells that also expressed GFAP, as previously reported after SCI (McTigue et al., 2001), were excluded from our analysis (please see details in Materials and Methods). It is important to note that since the CC1 antibody was produced in mouse, we observed non-specific staining from the IgGγ2B secondary antibody in and around the GFAP$^-$ lesion (Supplementary Fig. 1). Based on this region of non-specific staining, we omitted the 0–250μm distance from our analyses. In the uninjured spinal cord, the percentage of CC1$^+$tdTomato$^+$ cells was not significantly changed between genotypes at either 1 and 4 weeks after STAT3 or SOCS3 deletion in NG2 cells (Fig. 8S–T). At 1 week after SCI, the percentage of NG2 cells that differentiated into oligodendrocytes was significantly increased in WT and NG2-SOCS3 KO mice, but not in NG2-STAT3 KO mice as compared to uninjured controls (Fig. 8S). While SOCS3 deletion did not affect the percentage of CC1$^+$tdTomato$^+$ cells after SCI as compared to WT, there was a significant decrease after STAT3 deletion a week after injury (Fig. 8S). However, this difference was not maintained at 4 weeks where all three genotypes had similar percentages of CC1$^+$tdTomato$^+$ cells after SCI (Fig. 8T). It is important to note that due to the increased proliferation after SOCS3 deletion, the density of CC1$^+$tdTomato$^+$ cells was increased in the NG2-SOCS3 KO mice at 1 and 4 weeks after SCI (Supplementary Fig. 2) even though the percentage was not affected. Taken together, our data indicate that STAT3, rather than SOCS3, is necessary for early oligodendrogenesis after SCI.

To determine the role of the STAT3/SOCS3 on NG2 cell differentiation into astrocytes, we quantified the percentage of tdTomato$^+$ cells that colocalized with GFAP in WT (Fig 9G–R), NG2-STAT3 KO (Fig 9D–F), and NG2-SOCS3 KO mice (Fig. 9A–C). In the uninjured spinal cord (Fig. 9P–R, S–T)), we did not detect any GFAP$^+$tdTomato$^+$ cells in any of the three genotypes tested. While the percent of GFAP$^+$tdTomato$^+$ cells was increased in all three genotypes after SCI, it was not significantly different between the three groups at 1 or 4 weeks after SCI (Fig. 9S–T). Although the percentage was not different, the density of GFAP$^+$tdTomato$^+$ cells was increased after SOCS3 deletion (Supplementary Fig. 2), presumably due to the corresponding increased proliferation. Taken together, our data indicate that neither STAT3 nor SOCS3 deletion affects astrogliogenesis from NG2 cell after SCI.

Discussion

In this study, we sought to determine the role of STAT3 in NG2 cell proliferation and differentiation by generating NG2 cell specific deletion of STAT3 or its suppressor SOCS3 and using genetic fate mapping techniques after SCI. We showed that after SCI, STAT3 deletion leads to a reduction in oligodendrogenesis, and SOCS3 deletion leads to increased proliferation of NG2 cells within the glial scar. These non-opposing effects of STAT3 and SOCS3 suggest an independent role for these molecules in NG2 cell differentiation and proliferation after SCI. Although STAT3 and SOCS3 have been implicated in astrogliogenesis from neural stem cells, surprisingly they did not affect astrogliogenesis from NG2 cells after SCI. Altogether, our data demonstrate that STAT3 and SOCS3 are regulators of oligodendrogenesis and NG2 cell proliferation, respectively, after SCI.

Regulation of NG2 cell proliferation by STAT3/SOCS3

In the uninjured spinal cord, the density of NG2 lineage cells did not change between 1 and 4 weeks after tamoxifen injection, consistent with previous reports that NG2 cell density is maintained in the adult spinal cord (Kang et al., 2010). The density of NG2 lineage cells is markedly increased by 1 week after SCI, and is maintained at 4 weeks after SCI, consistent with previous reports that the majority of NG2 cell proliferation occurs within 7 days after SCI (Lytle et al., 2009, Lytle and Wrathall, 2007, McTigue et al., 2001, Zai and Wrathall, 2005). We also observed that the density of NG2 cells in the uninjured spinal cord was not altered by either STAT3 or SOCS3 deletion, which is likely due to low levels of cytokines such as CNTF and LIF in the uninjured adult spinal cord (Tripathi and McTigue, 2008, Zai et al., 2005).

We found that deletion of SOCS3 increased the proliferation of NG2 cells after SCI, which demonstrates a role for SOCS3 in regulating proliferation of NG2 cells after SCI. This could be important because NG2 cells have been reported to inhibit axon regeneration by shedding of the chondroitin sulfate proteoglycan NG2 as well as formation of synapses with dystrophic axons, thereby resulting in axonal entrapment (Dou and Levine, 1994, Filous et al., 2014, Petrosyan et al., 2013, Tan et al., 2006, Tan et al., 2005). Since we did not observe a change in density of NG2 lineage cells after STAT3 deletion, we did not perform proliferation and survival assays in this group. This lack of an effect was surprising given that the best described cytokines affecting NG2 cell proliferation and differentiation, such as CNTF and LIF, signal through the gp130-STAT3 pathway. Nonetheless, our data suggests that STAT3 is not involved or can be compensated by alternative signaling mechanisms that remain to be elucidated.

The use of a NG2-CreER line with a relatively low recombination efficiency (~30%) was advantageous for our lineage tracing studies, but it is possible that the remaining 70% of NG2 cells masked any functional effects of SOCS3 deletion in the minor NG2 cell population. These functional roles could have included detrimental effects on axon regeneration (Levine, 2015, Son, 2015) but also beneficial roles on neuroprotection such as those reported after SOCS3 deletion in astrocytes (Okada et al., 2006). Same holds true for the effects of STAT3 deletion; the initial reduction of oligodendrocytes after STAT3 deletion could have had more pronounced long-term effects on both pathology and behavior

if STAT3 was deleted in a majority of the NG2 cells. Thus, future studies will need to address the functional significance of increased NG2 cell proliferation after SOCS3 or decreased oligodendrogenesis with STAT3 deletion using a mouse line with higher recombination efficiency in NG2 cells.

The best described role of SOCS3 is suppression of STAT3 signaling, so we hypothesized that STAT3 and SOCS3 would have opposing effects. However, our data show that SOCS3 may have STAT3-independent roles in NG2 cells after SCI. SOCS3 has also been implicated in regulating other signaling pathways, such as IGF1/insulin, and TNFα/NFκB (Rottenberg and Carow, 2014), both of which are pathways known to be activated after SCI. Both IGF1 and TNFα have been shown to be important for the proliferation and subsequent differentiation ofNG2 cells after demyelination (Arnett et al., 2001, Mason et al., 2003). Overall, we have identified a novel non-canonical role for SOCS3 in NG2 cells after SCI, but detailed molecular mechanism remains to be investigated.

Regulation of NG2 cell differentiation by STAT3/SOCS3

In our studies, STAT3 deletion led to a reduction in oligodendrogenesis from NG2 cells after SCI. However, this reduction was short lived since at four weeks the percentage of oligodendrocytes was similar between the different groups. One possible explanation is that STAT3 deletion simply delays oligodendrogenesis after SCI. For example, both CNTF KO (Barres et al., 1996) and LIF KO mice (Ishibashi et al., 2009) have a developmental delay in oligodendrogenesis, but by adulthood reach normal levels of oligodendrocytes and myelination. Interestingly, SOCS3 deletion did not affect the percentage of NG2 cells differentiating into oligodendrocytes, suggesting that STAT3 is not regulated by SOCS3 in adult spinal cord NG2 cells or that increased STAT3 activation is not sufficient to increase oligodendrogenesis after SCI.

An interesting finding in our study was that STAT3/SOCS3 did not affect astrogliogenesis from NG2 cells after SCI. In neural stem cells, STAT3 activation leads to their differentiation into astrocytes, but only at certain developmental stages due to the methylation, and histone acetylation states of the STAT3 binding sites in the GFAP promoter (Kanski et al., 2014, Urayama et al., 2013). It is possible that adult spinal cord NG2 cells use a STAT3 independent mechanism to differentiate into astrocytes, or that, like neural stem cells, NG2 cells may differentiate into astrocytes in a specific epigenetic context. It would be interesting to determine whether NG2 cell derived astrogliogenesis seen during development is regulated by STAT3 and SOCS3.

Our data demonstrated that the percent of NG2 cell-derived astrocytes changed from approximately 25% at 1 week to approximately 8% at 4 weeks after SCI. This decline is consistent with a previous study (Komitova et al., 2011) where the authors proposed that a transient increase in GFAP expression in some NG2 cells could be a possible explanation. Alternatively, some NG2 cell-derived astrocytes may die after differentiation from NG2 cells. Lastly, the number of $GFAP^+$ cells derived from NG2 cells could remain the same while NG2 cells increase in number, but we believe that this is unlikely because our data shows that the density of NG2 cells remain constant between 1 and 4 weeks (Fig. 1). Since the percentage of oligodendrocytes remained constant between 1 and 4 weeks after SCI (Fig.

7), it is likely that the remaining tdTomato$^+$ cells are undifferentiated NG2 cells in the glial scar region, but more data is needed to support this possibility.

To our knowledge, this is the first study to investigate the role of STAT3 and SOCS3 in NG2 cells after CNS injury. Altogether, our data show that STAT3/SOCS3 are regulators of NG2 cell proliferation and differentiation in the glial scar region after contusive SCI. Interestingly, while STAT3/SOCS3 typically demonstrate opposing effects, they seem to have independent roles in regulating NG2 cell proliferation and differentiation after SCI. While SOCS3 regulates NG2 cell proliferation, STAT3 regulates oligodendrogenesis, and surprisingly, neither are necessary for astrogliogenesis by NG2 cells after SCI. This is in contrast to previous studies that have shown opposing effects of STAT3 and SOCS3 in astrocytes (Okada et al., 2006) and macrophages (Qin et al., 2012) after CNS injury. This non-canonical signaling mechanism by which STAT3 and SOCS3 regulate NG2 cells as well as their functional significance in recovery after SCI remains to be investigated further in the future.

Supplementary Material

Refer to Web version on PubMed Central for supplementary material.

Acknowledgments

We thank Dr. Kevin Park for the STAT3 and SOCS3 knockout mice and for insightful comments on our studies. This study was funded by NINDS R01NS081040, R21NS082835, US Army W81XWH131007715, The Miami Project to Cure Paralysis, and the Buoniconti Fund. A.R.H was funded by the Lois Pope LIFE Fellows Program. We thank Yadira Salgueiro, Yunjiao Zhu, Shaffiat Karmally, and Kirill Lyapichev for technical assistance and animal care. We thank Wolfgang Pita-Thomas for helpful comments. We thank Pernille Madsen and Michelle Trojanowsky for assistance with NG2 cell culture protocol.

Abbreviations

CNTF	Ciliary Neurotrophic Factor
CSPG	Chondroitin Sulfate Proteoglycan
DAPI	4′,6-diamidino-2-phenylindole
EdU	5-ethynyl-2′-deoxyuridine
GFAP	Glial Fibrillary Acidic Protein
JAK	Janus Kinase
LIF	Leukemia Inhibitory Factor
NG2	Neural Glial Antigen 2
OPC	Oligodendrocyte Progenitor Cell
SCI	Spinal Cord Injury
SOCS3	Suppressor of Cytokine Signaling 3
STAT3	Signal Transducer and Activator of Transcription 3

TUNEL Terminal Deoxynucleotidyl Transferase (TdT) dUTP Nick-End Labeling

References

Arenkiel BR, Hasegawa H, Yi JJ, Larsen RS, Wallace ML, Philpot BD, Wang F, Ehlers MD. Activity-induced remodeling of olfactory bulb microcircuits revealed by monosynaptic tracing. PLoS One. 2011; 6:e29423. [PubMed: 22216277]

Arnett HA, Mason J, Marino M, Suzuki K, Matsushima GK, Ting JP. TNF alpha promotes proliferation of oligodendrocyte progenitors and remyelination. Nat Neurosci. 2001; 4:1116–22. [PubMed: 11600888]

Barres BA, Burne JF, Holtmann B, Thoenen H, Sendtner M, Raff MC. Ciliary neurotrophic factor enhances the rate of oligodendrocyte generation. Mol Cell Neurosci. 1996; 8:146–56.

Bonni A, Sun Y, Nadal-Vicens M, Bhatt A, Frank DA, Rozovsky I, Stahl N, Yancopoulos GD, Greenberg ME. Regulation of gliogenesis in the central nervous system by the JAK-STAT signaling pathway. Science. 1997; 278:477–83. [PubMed: 9334309]

Bu J, Akhtar N, Nishiyama A. Transient expression of the NG2 proteoglycan by a subpopulation of activated macrophages in an excitotoxic hippocampal lesion. Glia. 2001; 34:296–310. [PubMed: 11360302]

Bugga L, Gadient RA, Kwan K, Stewart CL, Patterson PH. Analysis of neuronal and glial phenotypes in brains of mice deficient in leukemia inhibitory factor. J Neurobiol. 1998; 36:509–24. [PubMed: 9740023]

Dincman TA, Beare JE, Ohri SS, Whittemore SR. Isolation of cortical mouse oligodendrocyte precursor cells. J Neurosci Methods. 2012; 209:219–26. [PubMed: 22743801]

Dou CL, Levine JM. Inhibition of neurite growth by the NG2 chondroitin sulfate proteoglycan. J Neurosci. 1994; 14:7616–28. [PubMed: 7996200]

Filous AR, Tran A, Howell CJ, Busch SA, Evans TA, Stallcup WB, Kang SH, Bergles DE, Lee SI, Levine JM, Silver J. Entrapment via synaptic-like connections between NG2 proteoglycan+ cells and dystrophic axons in the lesion plays a role in regeneration failure after spinal cord injury. J Neurosci. 2014; 34:16369–84. [PubMed: 25471575]

Gavrieli Y, Sherman Y, Ben-Sasson SA. Identification of programmed cell death in situ via specific labeling of nuclear DNA fragmentation. J Cell Biol. 1992; 119:493–501. [PubMed: 1400587]

Goritz C, Dias DO, Tomilin N, Barbacid M, Shupliakov O, Frisen J. A pericyte origin of spinal cord scar tissue. Science. 2011; 333:238–42. [PubMed: 21737741]

Herrmann JE, Imura T, Song B, Qi J, Ao Y, Nguyen TK, Korsak RA, Takeda K, Akira S, Sofroniew MV. STAT3 is a critical regulator of astrogliosis and scar formation after spinal cord injury. J Neurosci. 2008; 28:7231–43. [PubMed: 18614693]

Hesp ZC, Goldstein EA, Miranda CJ, Kaspar BK, McTigue DM. Chronic oligodendrogenesis and remyelination after spinal cord injury in mice and rats. J Neurosci. 2015; 35:1274–90. [PubMed: 25609641]

Horner PJ, Power AE, Kempermann G, Kuhn HG, Palmer TD, Winkler J, Thal LJ, Gage FH. Proliferation and differentiation of progenitor cells throughout the intact adult rat spinal cord. J Neurosci. 2000; 20:2218–28. [PubMed: 10704497]

Ishibashi T, Lee PR, Baba H, Fields RD. Leukemia inhibitory factor regulates the timing of oligodendrocyte development and myelination in the postnatal optic nerve. J Neurosci Res. 2009; 87:3343–55. [PubMed: 19598242]

Kang SH, Fukaya M, Yang JK, Rothstein JD, Bergles DE. NG2+ CNS glial progenitors remain committed to the oligodendrocyte lineage in postnatal life and following neurodegeneration. Neuron. 2010; 68:668–81. [PubMed: 21092857]

Kanski R, Sneeboer MA, van Bodegraven EJ, Sluijs JA, Kropff W, Vermunt MW, Creyghton MP, De Filippis L, Vescovi A, Aronica E, van Tijn P, van Strien ME, Hol EM. Histone acetylation in astrocytes suppresses GFAP and stimulates a reorganization of the intermediate filament network. J Cell Sci. 2014; 127:4368–80. [PubMed: 25128567]

Komitova M, Serwanski DR, Lu QR, Nishiyama A. NG2 cells are not a major source of reactive astrocytes after neocortical stab wound injury. Glia. 2011; 59:800–9. [PubMed: 21351161]

Lee DH, Lee JK. Animal models of axon regeneration after spinal cord injury. Neurosci Bull. 2013; 29:436–44. [PubMed: 23893429]

Lee JK, Case LC, Chan AF, Zhu Y, Tessier-Lavigne M, Zheng B. Generation of an OMgp allelic series in mice. Genesis. 2009; 47:751–6. [PubMed: 19672953]

Levine J. The reactions and role of NG2 glia in spinal cord injury. Brain Res. 2015

Levine JM. Increased expression of the NG2 chondroitin-sulfate proteoglycan after brain injury. J Neurosci. 1994; 14:4716–30. [PubMed: 8046446]

Liu XZ, Xu XM, Hu R, Du C, Zhang SX, McDonald JW, Dong HX, Wu YJ, Fan GS, Jacquin MF, Hsu CY, Choi DW. Neuronal and glial apoptosis after traumatic spinal cord injury. J Neurosci. 1997; 17:5395–406. [PubMed: 9204923]

Lytle JM, Chittajallu R, Wrathall JR, Gallo V. NG2 cell response in the CNP-EGFP mouse after contusive spinal cord injury. Glia. 2009; 57:270–85. [PubMed: 18756526]

Lytle JM, Wrathall JR. Glial cell loss, proliferation and replacement in the contused murine spinal cord. Eur J Neurosci. 2007; 25:1711–24. [PubMed: 17432960]

Mason JL, Xuan S, Dragatsis I, Efstratiadis A, Goldman JE. Insulin-like growth factor (IGF) signaling through type 1 IGF receptor plays an important role in remyelination. J Neurosci. 2003; 23:7710–8. [PubMed: 12930811]

Mayer M, Bhakoo K, Noble M. Ciliary neurotrophic factor and leukemia inhibitory factor promote the generation, maturation and survival of oligodendrocytes in vitro. Development. 1994; 120:143–53. [PubMed: 8119123]

McTigue DM, Tripathi R, Wei P. NG2 colocalizes with axons and is expressed by a mixed cell population in spinal cord lesions. J Neuropathol Exp Neurol. 2006; 65:406–20. [PubMed: 16691121]

McTigue DM, Wei P, Stokes BT. Proliferation of NG2-positive cells and altered oligodendrocyte numbers in the contused rat spinal cord. J Neurosci. 2001; 21:3392–400. [PubMed: 11331369]

Moh A, Iwamoto Y, Chai GX, Zhang SS, Kano A, Yang DD, Zhang W, Wang J, Jacoby JJ, Gao B, Flavell RA, Fu XY. Role of STAT3 in liver regeneration: survival, DNA synthesis, inflammatory reaction and liver mass recovery. Lab Invest. 2007; 87:1018–28. [PubMed: 17660847]

Mori H, Hanada R, Hanada T, Aki D, Mashima R, Nishinakamura H, Torisu T, Chien KR, Yasukawa H, Yoshimura A. Socs3 deficiency in the brain elevates leptin sensitivity and confers resistance to diet-induced obesity. Nat Med. 2004; 10:739–43. [PubMed: 15208705]

Nakashima K, Wiese S, Yanagisawa M, Arakawa H, Kimura N, Hisatsune T, Yoshida K, Kishimoto T, Sendtner M, Taga T. Developmental requirement of gp130 signaling in neuronal survival and astrocyte differentiation. J Neurosci. 1999a; 19:5429–34. [PubMed: 10377352]

Nakashima K, Yanagisawa M, Arakawa H, Kimura N, Hisatsune T, Kawabata M, Miyazono K, Taga T. Synergistic signaling in fetal brain by STAT3-Smad1 complex bridged by p300. Science. 1999b; 284:479–82. [PubMed: 10205054]

Nishiyama A, Komitova M, Suzuki R, Zhu X. Polydendrocytes (NG2 cells): multifunctional cells with lineage plasticity. Nat Rev Neurosci. 2009; 10:9–22. [PubMed: 19096367]

Okada S, Nakamura M, Katoh H, Miyao T, Shimazaki T, Ishii K, Yamane J, Yoshimura A, Iwamoto Y, Toyama Y, Okano H. Conditional ablation of Stat3 or Socs3 discloses a dual role for reactive astrocytes after spinal cord injury. Nat Med. 2006; 12:829–34. [PubMed: 16783372]

Petrosyan HA, Hunanyan AS, Alessi V, Schnell L, Levine J, Arvanian VL. Neutralization of inhibitory molecule NG2 improves synaptic transmission, retrograde transport, and locomotor function after spinal cord injury in adult rats. J Neurosci. 2013; 33:4032–43. [PubMed: 23447612]

Pfeifer A, Brandon EP, Kootstra N, Gage FH, Verma IM. Delivery of the Cre recombinase by a self-deleting lentiviral vector: efficient gene targeting in vivo. Proc Natl Acad Sci U S A. 2001; 98:11450–5. [PubMed: 11553794]

Qin H, Yeh WI, De Sarno P, Holdbrooks AT, Liu Y, Muldowney MT, Reynolds SL, Yanagisawa LL, Fox TH 3rd, Park K, Harrington LE, Raman C, Benveniste EN. Signal transducer and activator of transcription-3/suppressor of cytokine signaling-3 (STAT3/SOCS3) axis in myeloid cells regulates neuroinflammation. Proc Natl Acad Sci U S A. 2012; 109:5004–9. [PubMed: 22411837]

Rottenberg ME, Carow B. SOCS3, a major regulator of infection and inflammation. Frontiers in Immunology. 2014; 5

Sellers DL, Maris DO, Horner PJ. Postinjury niches induce temporal shifts in progenitor fates to direct lesion repair after spinal cord injury. J Neurosci. 2009; 29:6722–33. [PubMed: 19458241]

Soderblom C, Luo X, Blumenthal E, Bray E, Lyapichev K, Ramos J, Krishnan V, Lai-Hsu C, Park KK, Tsoulfas P, Lee JK. Perivascular fibroblasts form the fibrotic scar after contusive spinal cord injury. J Neurosci. 2013; 33:13882–7. [PubMed: 23966707]

Son YJ. Synapsing with NG2 cells (polydendrocytes), unappreciated barrier to axon regeneration? Neural Regen Res. 2015; 10:346–8. [PubMed: 25878571]

Srinivas S, Watanabe T, Lin CS, William CM, Tanabe Y, Jessell TM, Costantini F. Cre reporter strains produced by targeted insertion of EYFP and ECFP into the ROSA26 locus. BMC Dev Biol. 2001; 1:4. [PubMed: 11299042]

Tan AM, Colletti M, Rorai AT, Skene JH, Levine JM. Antibodies against the NG2 proteoglycan promote the regeneration of sensory axons within the dorsal columns of the spinal cord. J Neurosci. 2006; 26:4729–39. [PubMed: 16672645]

Tan AM, Zhang W, Levine JM. NG2: a component of the glial scar that inhibits axon growth. J Anat. 2005; 207:717–25. [PubMed: 16367799]

Tripathi RB, McTigue DM. Chronically increased ciliary neurotrophic factor and fibroblast growth factor-2 expression after spinal contusion in rats. J Comp Neurol. 2008; 510:129–44. [PubMed: 18615534]

Tripathi RB, Rivers LE, Young KM, Jamen F, Richardson WD. NG2 glia generate new oligodendrocytes but few astrocytes in a murine experimental autoimmune encephalomyelitis model of demyelinating disease. J Neurosci. 2010; 30:16383–90. [PubMed: 21123584]

Urayama S, Semi K, Sanosaka T, Hori Y, Namihira M, Kohyama J, Takizawa T, Nakashima K. Chromatin accessibility at a STAT3 target site is altered prior to astrocyte differentiation. Cell Struct Funct. 2013; 38:55–66. [PubMed: 23439558]

Wanner IB, Anderson MA, Song B, Levine J, Fernandez A, Gray-Thompson Z, Ao Y, Sofroniew MV. Glial scar borders are formed by newly proliferated, elongated astrocytes that interact to corral inflammatory and fibrotic cells via STAT3-dependent mechanisms after spinal cord injury. J Neurosci. 2013; 33:12870–86. [PubMed: 23904622]

Zai LJ, Wrathall JR. Cell proliferation and replacement following contusive spinal cord injury. Glia. 2005; 50:247–57. [PubMed: 15739189]

Zai LJ, Yoo S, Wrathall JR. Increased growth factor expression and cell proliferation after contusive spinal cord injury. Brain Res. 2005; 1052:147–55. [PubMed: 16005441]

Zawadzka M, Rivers LE, Fancy SP, Zhao C, Tripathi R, Jamen F, Young K, Goncharevich A, Pohl H, Rizzi M, Rowitch DH, Kessaris N, Suter U, Richardson WD, Franklin RJ. CNS-resident glial progenitor/stem cells produce Schwann cells as well as oligodendrocytes during repair of CNS demyelination. Cell Stem Cell. 2010; 6:578–90. [PubMed: 20569695]

Zhu X, Hill RA, Dietrich D, Komitova M, Suzuki R, Nishiyama A. Age-dependent fate and lineage restriction of single NG2 cells. Development. 2011; 138:745–53. [PubMed: 21266410]

Zhu Y, Soderblom C, Trojanowsky M, Lee DH, Lee JK. Fibronectin Matrix Assembly after Spinal Cord Injury. J Neurotrauma. 2015; 32:1158–67. [PubMed: 25492623]

Highlights

- NG2 cell proliferation is regulated by SOCS3 whereas their differentiation into oligodendrocytes is regulated by STAT3 after spinal cord injury
- Neither STAT3 nor SOCS3 deletion affects NG2 cell differentiation into astrocytes after spinal cord injury

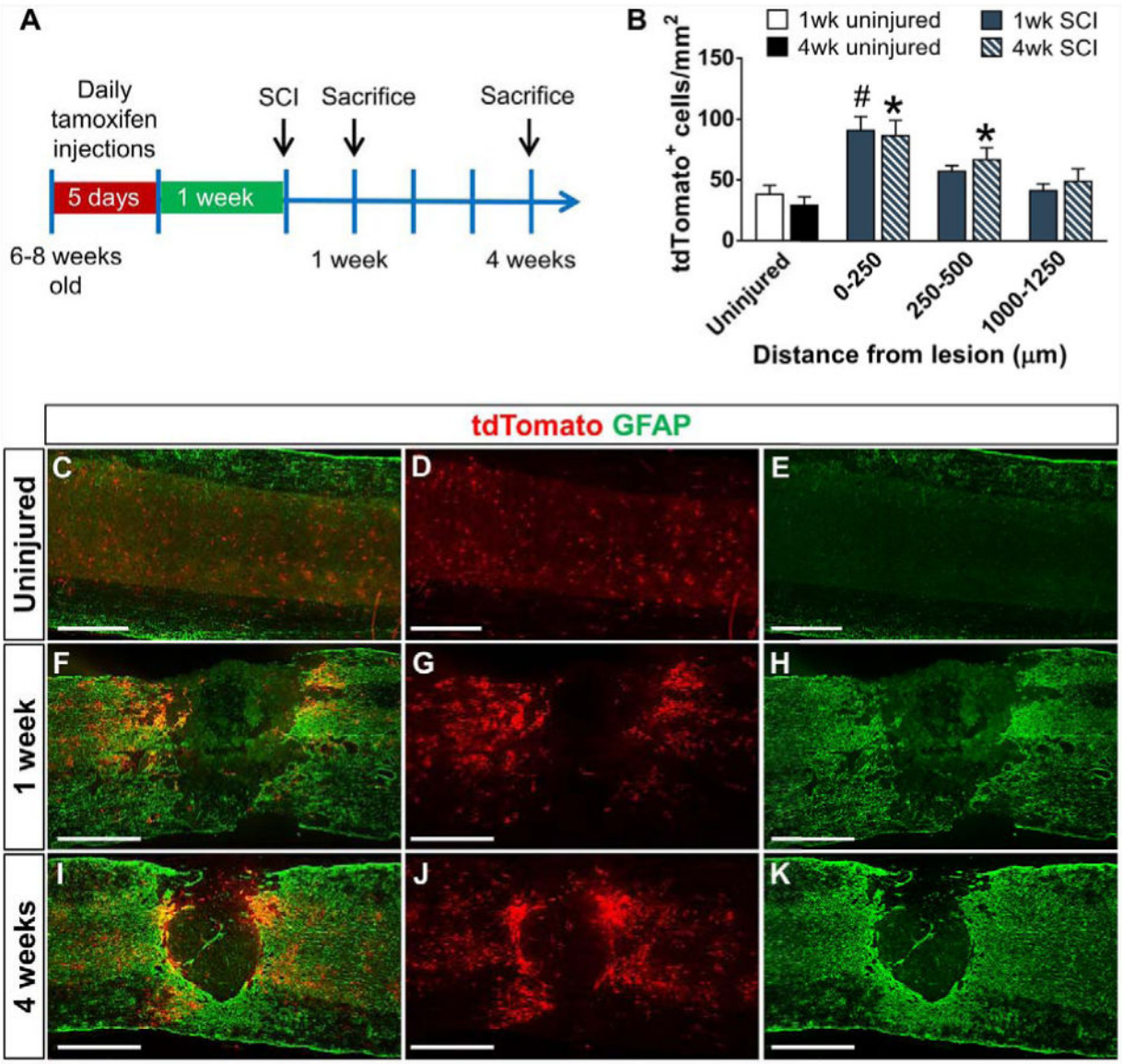

Figure 1. NG2 lineage cells within the glial scar increase in density after SCI

(A) Schematic describing the genetic lineage tracing experiment for NG2 cells. tdTomato-labeled NG2 cells and their progeny (red) are evenly distributed within the uninjured spinal cord **(C–E)** but aggregate around the injury site within the GFAP$^+$ glial scar (green) at 1 week **(F–H)** and 4 weeks **(I–K)** after contusive SCI. Quantification of the density and distribution of tdTomato$^+$ cells in the uninjured and injured spinal cord indicates an increase in the glial scar region **(B)**. n=5 animals for all SCI groups and n=4 for uninjured groups. #p<0.05 compared to 1 week uninjured group. *p<0.05 compared to 4 week uninjured group. Two-way ANOVA with Tukey's multiple comparisons *post hoc* test. All images are from sagittal spinal cord sections. Scale bar=500 μm.

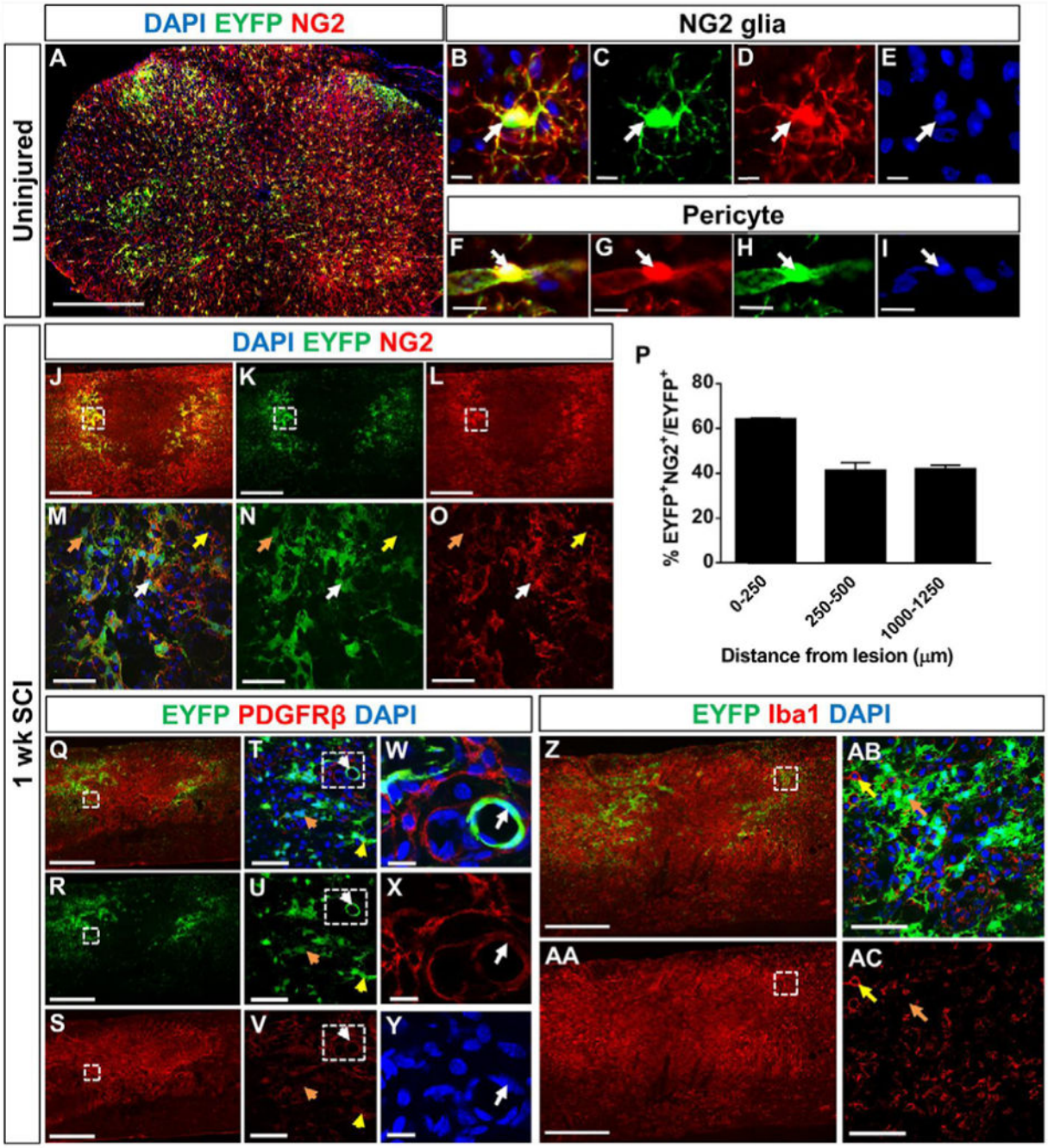

Figure 2. Reporter labeled cells in the glial scar are predominately NG2$^+$ glia

EYFP-labeled cells make up about 30% of NG2$^+$ cells **(A)**, which are comprised of both NG2$^+$ glia **(B–E)** and pericytes **(F–I, W–Y)**. The image in **(A)** is a coronal section from an uninjured spinal cord of NG2-EYFP mice one day after the last tamoxifen injection. 40–60% of EYFP$^+$ cells within the glial scar colocalize with NG2 at 1 week after SCI **(J–P**, white arrows indicates colocalization, orange arrows indicate non-colocalization**)**. NG2$^+$ cells that resemble round macrophages are not EYFP$^+$ **(**yellow arrows in **M–O)**. PDGFRβ$^+$ pericytes are present in the lesion core **(Q–S)**, and almost all of them are EYFP negative **(Q–**

Y, orange arrows in **T–V)**. Most of the EYFP$^+$ cells that colocalize with PDGFRβ had pericyte morphology **(**white arrows in **W–Y)**, with rare exceptions **(**yellow arrows in **T–V)**. EYFP$^+$ cells never colocalize with the macrophages/microglia marker Iba1 **(Z–AA)**. The yellow arrows in **(AB–AC)** represent an Iba1$^+$ macrophage not colocalizing with EYFP, and the orange arrows represents an EYFP$^+$ cell not colocalizing with Iba1. Scale bar=500 μm for **(A, J–L, Q–S, Z-AA)**, scale bar=10 μm for **(B–I, W–Y)**, and scale bar=50 μm for **(M–O, W–Y, AB–AC). (M–O)** are magnified views of dashed region in **(J–L). (T–V)** are magnified views of dashed region in **(Q–S). (W–Y)** are magnified views of dashed region in **(T–V). (AB–AC)** are magnified views of dashed region in **(Z-AA).** Images **(J–O, Q-AC)** are from sagittal spinal cord sections. n=3 animals.

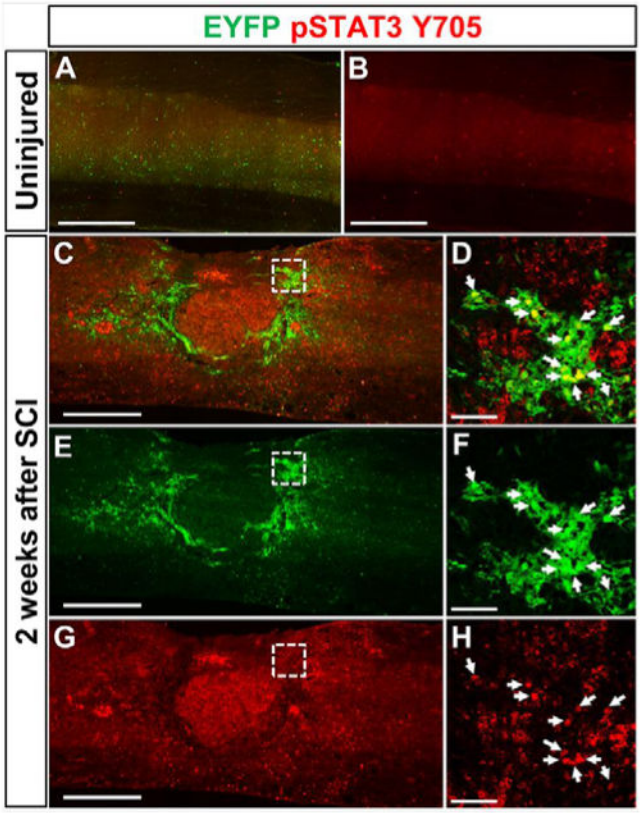

Figure 3. NG2 lineage cells express phosphorylated STAT3 after SCI

In the uninjured spinal cord **(A–B)**, levels of phosphorylated STAT3 (red) are undetectable immunohistochemically. However, 2 weeks after contusive SCI **(C–H)** phosphorylated STAT3 is detected within $EYFP^{+}$ NG2 lineage cells (green) that surround the lesion. **(D, F, H)** are magnified views of dashed region in **(C, E, G).** White arrows indicate colocalization. Scale bar=500 μm for **(C, E, G)**. Scale bar=50 μm for **(D, F, H)**.

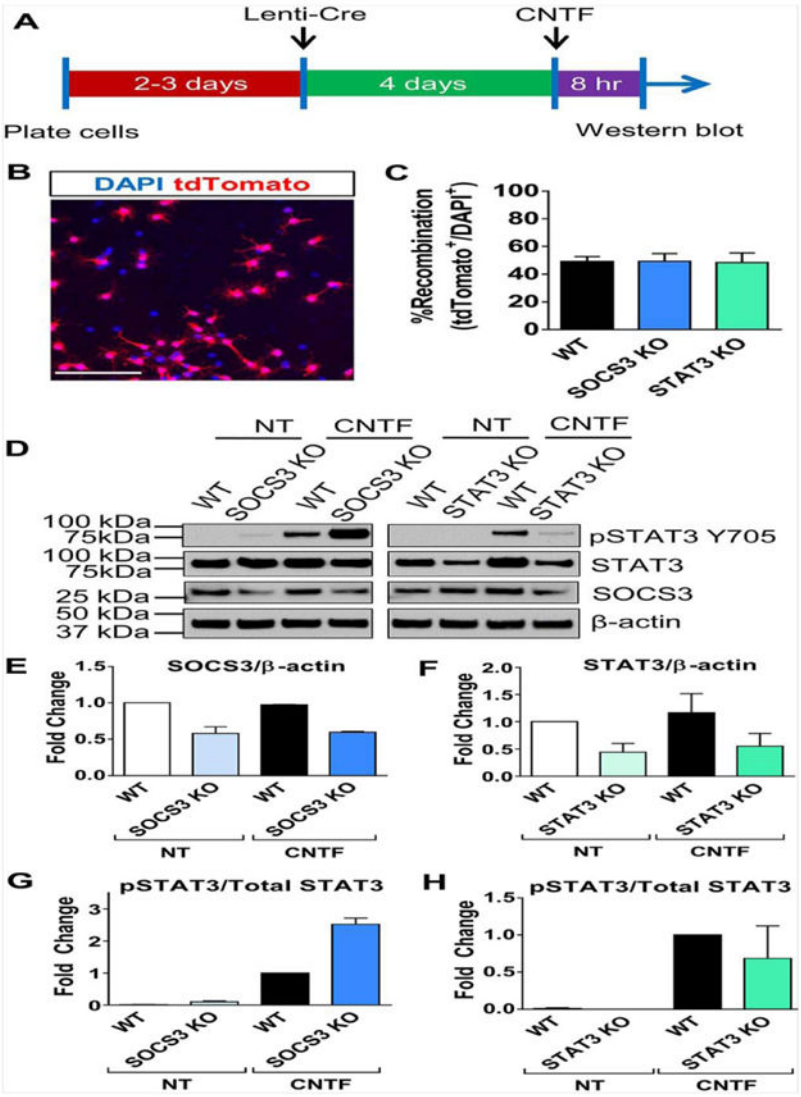

Figure 4. Confirmation of STAT3/SOCS3 deletion in primary NG2 cells

Experimental schematic for inducing recombination in primary NG2 cells **(A).** Transduction of primary NG2 cells from WT, SOCS3 KO or STAT3 KO mice (each carrying Rosa26-tdTomato allele) with Lenti-Cre induces tdTomato expression in approximately 50% of total cell population **(B, C)**. Representative western blot of WT, SOCS3 KO, or STAT3 KO mouse primary NG2 cells with no treatment (NT) or treatment with ciliary neurotrophic factor (CNTF) **(D)**. Quantification of Western blot showed reduction of SOCS3 in the SOCS3 KO cells **(E)** and reduction of STAT3 in the STAT3 KO cells **(F)**. Each group was normalized to WT cells with no treatment in **(E–F)**. It is important to note that residual STAT3/SOCS3 expression in KO cells is likely due to recombination in only a subpopulation of NG2 cells. Quantification of Western blot showed increased phospho-STAT3 (relative to total STAT3) in SOCS3 KO cells after CNTF treatment **(G)** while it remained unchanged in STAT3 KO cells **(H)**. Each group was normalized to WT with CNTF treatment in **(G–H)**. Quantification of **(E–H)** is from two western blots from two separate experiments. Scale bar in B=100 μm.

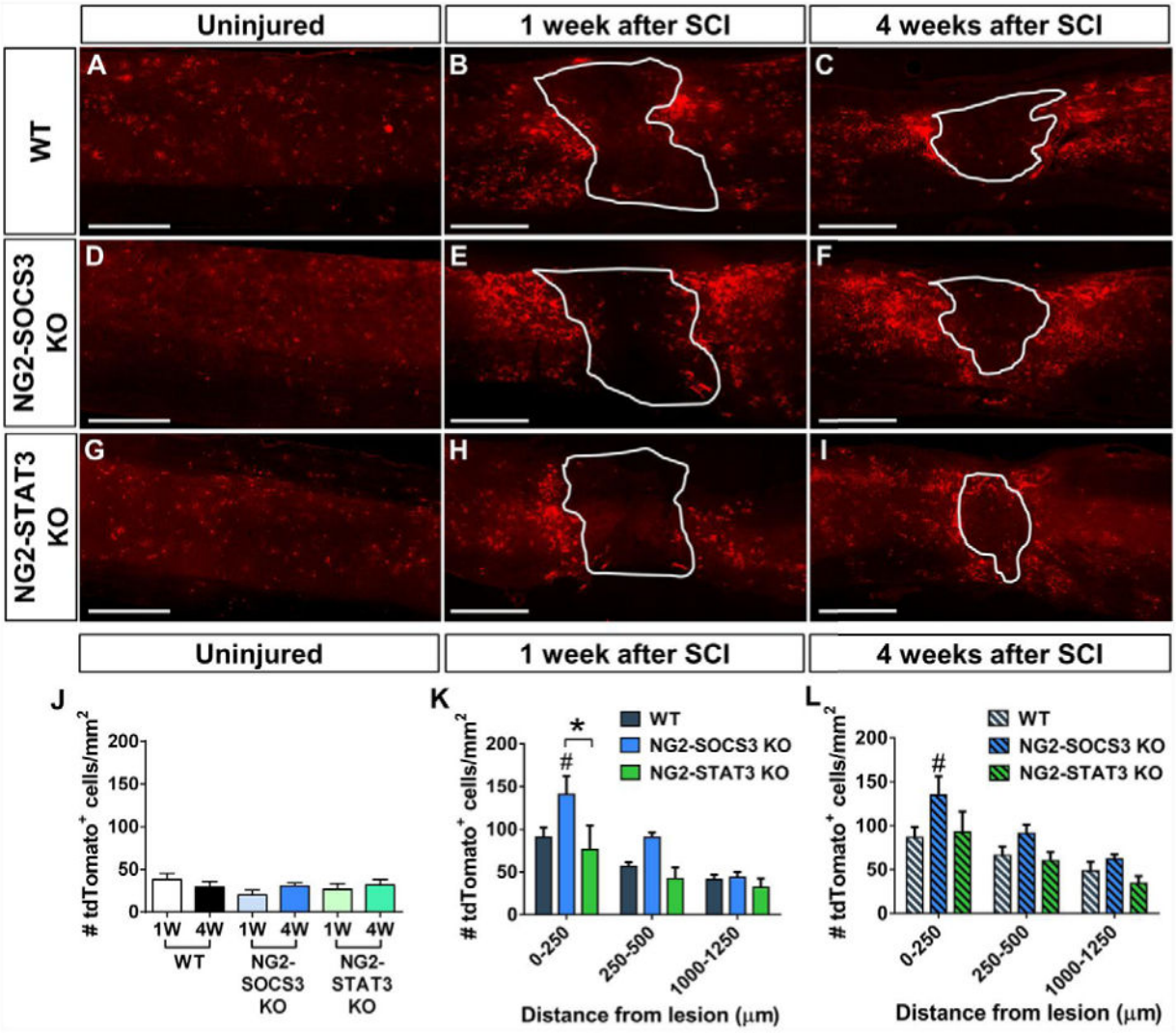

Figure 5. SOCS3 but not STAT3 deletion increases NG2 lineage cell number within the glial scar after SCI

Sagittal spinal cord sections showing a similar distribution of tdTomato$^+$ cells in the uninjured spinal cord from WT **(A, J)**, NG2-SOCS3 KO **(D, J)**, and NG2-STAT3 KO **(G, J)** mice. At both 1 week **(B, E, H, K)** and 4 weeks **(C, F, I, L)** after SCI, there is an increased number of tdTomato$^+$ cells adjacent to the lesion in NG2-SOCS3 KO mice. Region enclosed by solid line represents the lesion site as defined by the GFAP negative region (not shown). n=5 animals for all groups. #p<0.05 compared to WT. *p<0.05 comparing the two bracketed bars. Two-way ANOVA with repeated measures and Tukey's multiple comparisons *post hoc* test. Scale bar=500 μm.

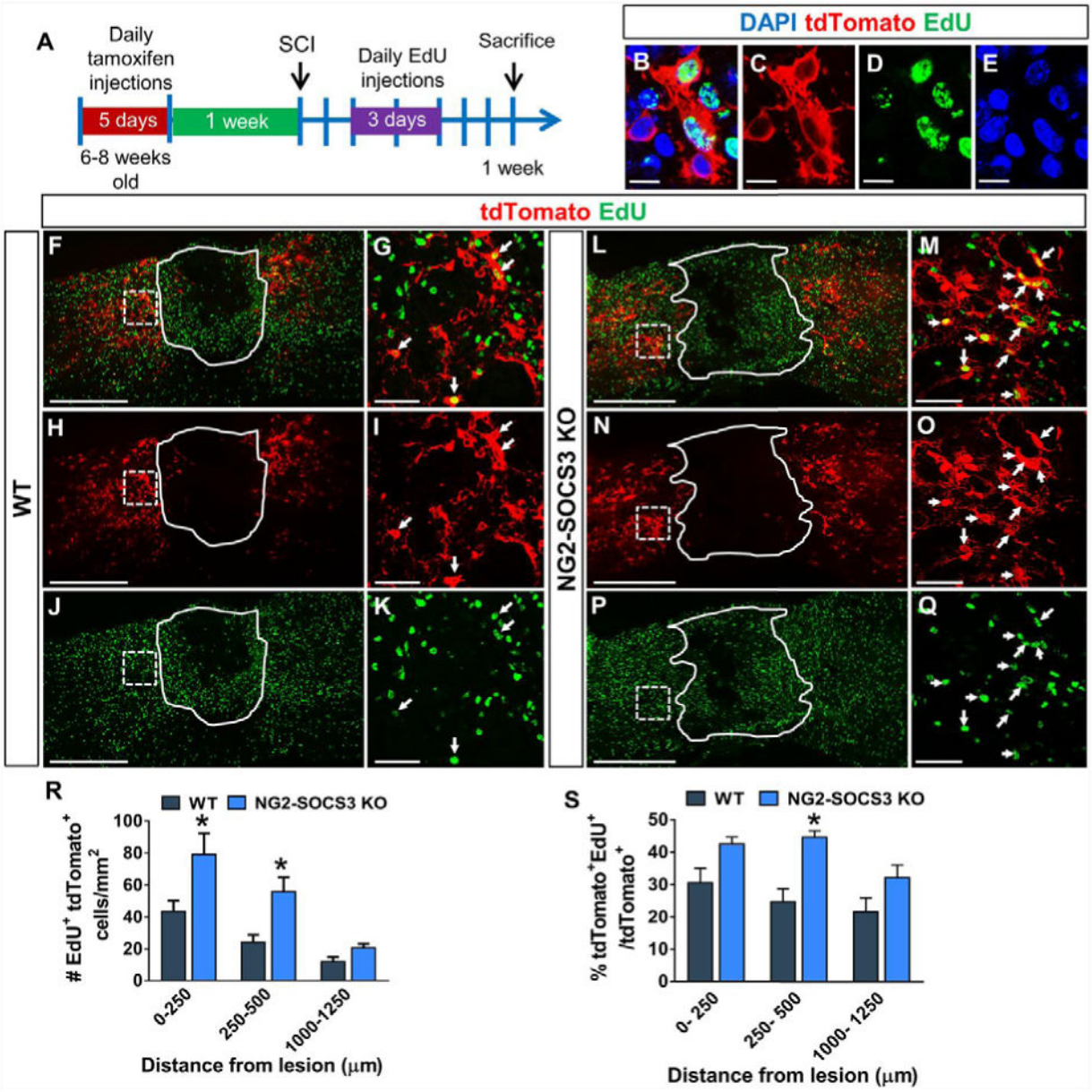

Figure 6. SOCS3 deletion increases NG2 cell proliferation within the glial scar after SCI

(A) Schematic describing the EdU incorporation experiment. **(B–E)** EdU^+ cells are $DAPI^+$. At 1 week after SCI, NG2-SOCS3 KO mice **(L–Q)** show greater number **(R)** and percent **(S)** of $tdTomato^+$ cells that are also EdU^+ near the injury site as compared to WT mice **(F–K)**. Region enclosed by solid line represents the lesion site as defined by the $GFAP^-$ area (not shown). **(G, I, K)** are magnified views of regions enclosed by dashed lines in **(F, H, J)**. **(M, O, Q)** are magnified views of regions enclosed by dashed lines in **(L, N, P)**. White arrows in **(G, I, K, M, O, Q)** indicate colocalization. *$p<0.05$ compared to WT at each corresponding region. Two-way ANOVA with repeated measures and Tukey's multiple comparisons *post hoc* test. All images are from sagittal spinal cord sections. n=5 animals for

WT and n=6 for NG2-SOCS3 KO. Scale bar=500 μm for **(F, H, J, L, N, P)**. Scale bar=50 μm for **(G, I, K, M, O, Q)**. Scale bar=10 μm for **(B–E)**.

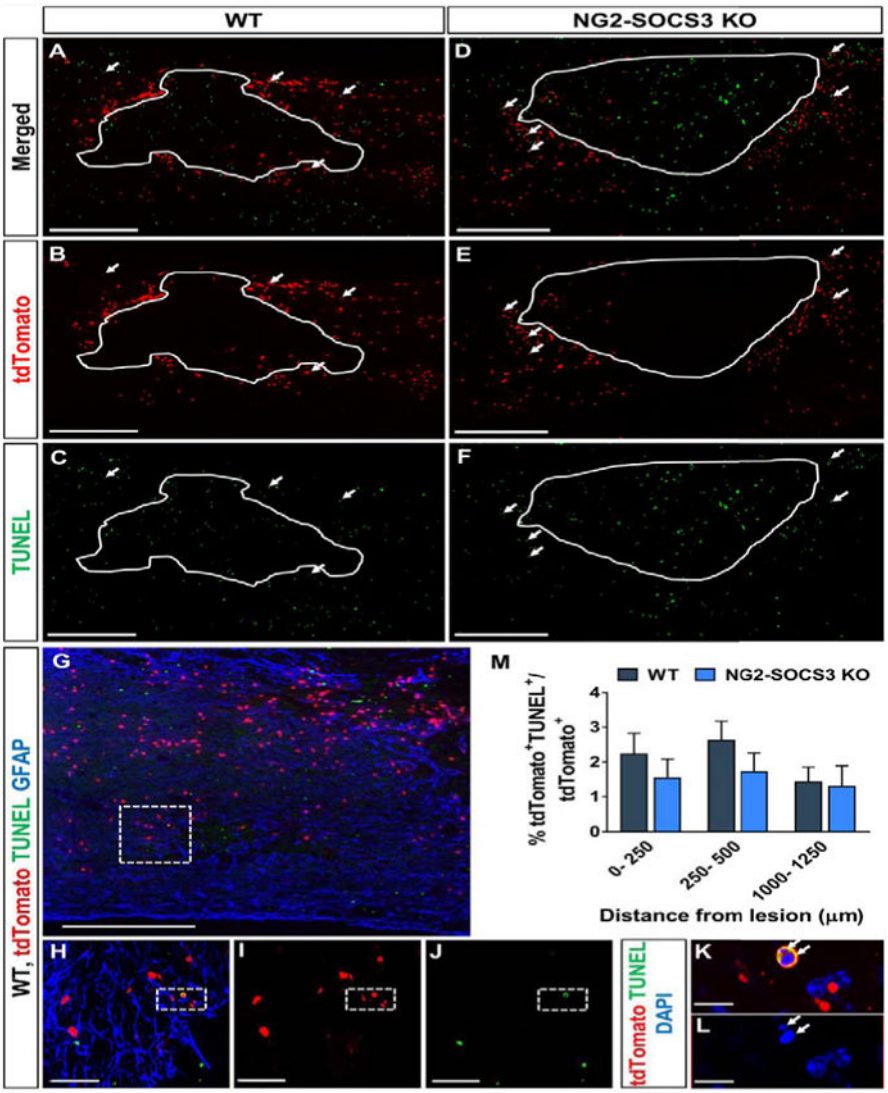

Figure 7. SOCS3 deletion does not affect NG2 cell survival within the glial scar after SCI

The percent of tdTomato$^+$ cells that were also TUNEL$^+$ was not significantly different between WT **(A–C, G–L)** and NG2-SOCS3 KO mice **(D–F)** at 1 week after SCI **(M)**. Area enclosed by solid line represents the lesion site as defined by the GFAP$^-$ area (not shown). **(K, L)** are magnified views of dashed region in **(H–J)**, which are magnified views of the dashed region in **(G)**. White arrows indicate TUNEL$^+$ tdTomato$^+$ cells **(K, L)**. One-way ANOVA with repeated measures and Tukey's multiple comparisons *post hoc* test. Scale bar=500μm for (A–G). Scale bar=50 μm for **(H–J)**. Scale bar=10 μm for **(K–L)**.

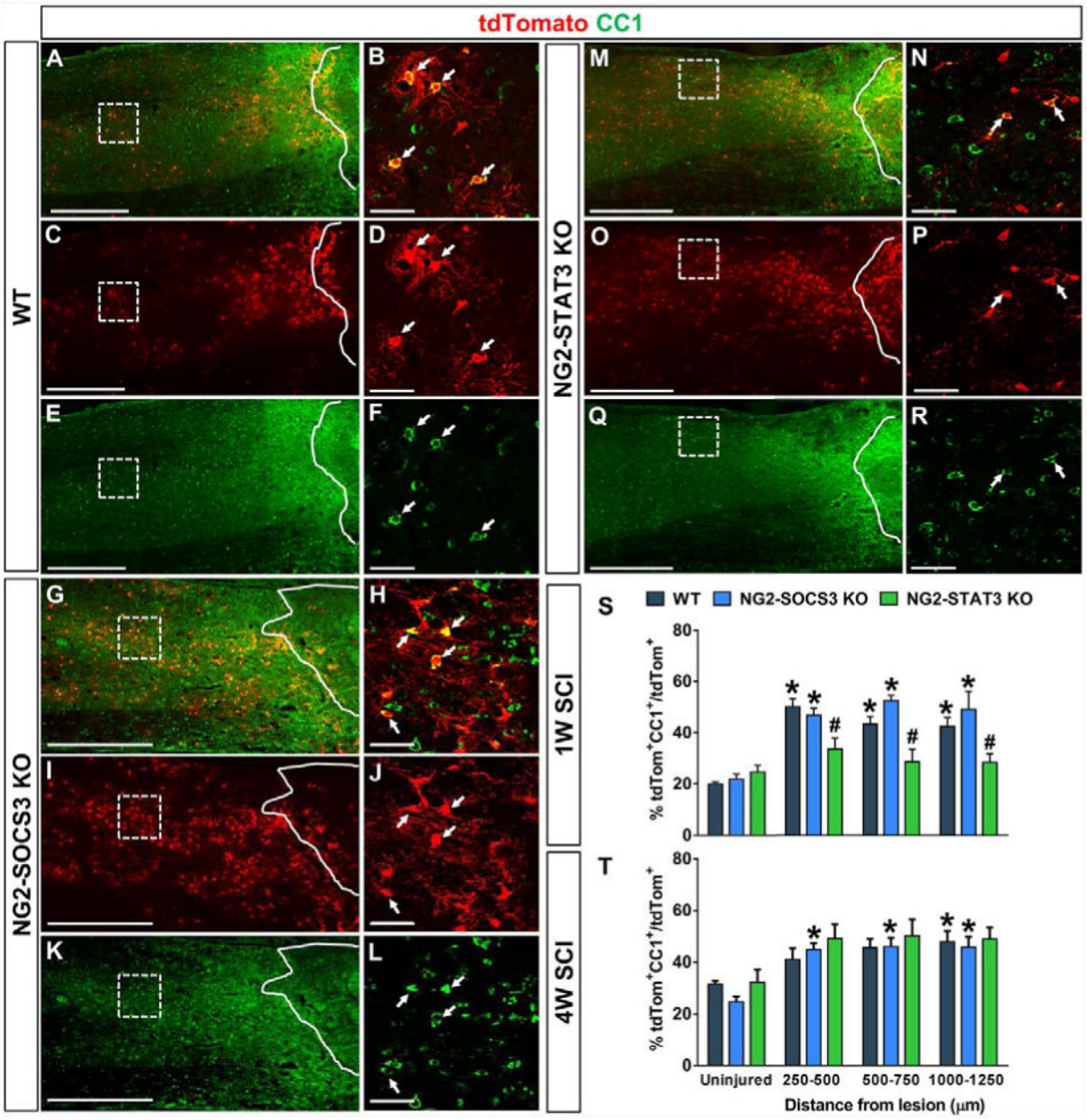

Figure 8. STAT3 deletion decreases differentiation of NG2 cells into oligodendrocytes

In the uninjured spinal cord, the percent of tdTomato$^+$ cells that are also CC1$^+$ are not significantly different between WT, NG2-SOCS3 KO, and NG2-STAT3 KO mice **(S–T)**. One week after SCI **(S)**, the percentage of tdTomato$^+$ cells that differentiate into mature oligodendrocytes significantly increases compared to the uninjured levels in the WT and NG2-SOCS3 KO but not the NG2-STAT3 KO mice. Compared to WT **(A–F)**, there was a decrease in percentage of tdTomato$^+$ cells that were also CC1$^+$ in the NG2-STAT3 KO mice **(M–R, S)**, while NG2-SOCS3 KO mice **(G–L, S)** remained similar to WT mice **(A–F, S)**. At 4 weeks after SCI **(T)**, the percentages of CC1$^+$ tdTomato$^+$ cells is not different between any of the genotypes. Regions enclosed by solid lines represent lesion site defined as the

GFAP^{-} region (not shown). Regions enclosed by dashed lines is magnified in the panel on the right side. White arrows indicate colocalization. n=5 animals for all groups. #p<0.05 compared to WT in each corresponding distance. Two-way ANOVA with repeated measures and Tukey's multiple comparisons *post hoc* test. *p<0.05 compared between uninjured and injured within the same genotype. One-way ANOVA with Tukey's multiple comparisons *post hoc* test. Scale bar=500 μm for **(A, C, E, G, I, K, M, O, Q)** and Scale bar=50 μm for **(B, D, F, H, J, L, N, P, R)**.

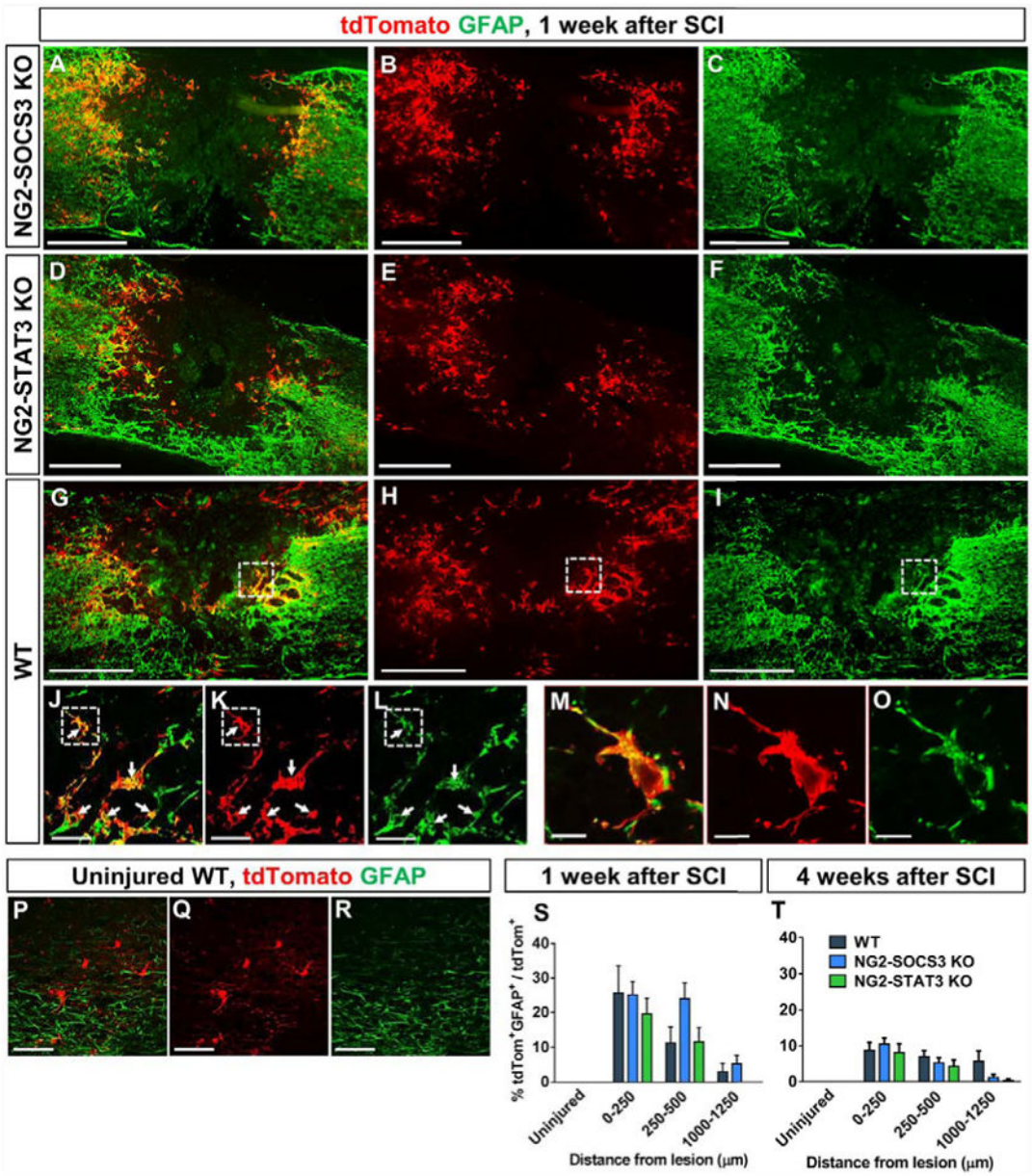

Figure 9. Neither STAT3 nor SOCS3 are required for NG2 cells to differentiate into GFAP$^+$ astrocytes after SCI

NG2 lineage cells (tdTomato$^+$) do not express the astrocyte marker GFAP in the uninjured spinal cord **(P–T)**. However, a subpopulation becomes GFAP$^+$ by 1 week after SCI in both adjacent and distant regions from the lesion site **(S)**. These GFAP$^+$ NG2 lineage cells continue to be present at 4 weeks after SCI **(T**, images not shown**)**. All images are from sagittal spinal cord sections. **(M–O)** are magnified views of dotted region in **(J–L)** respectively. **(J–L)** are magnified views of the dashed region in **(G–I)** respectively. White arrows indicate colocalization. There was no difference between WT **(G–O)**, NG2-STAT3 **(D–F)** and NG2-SOCS3 KO mice **(A–C)** in the percentage of tdTomato$^+$ cells that colocalize with GFAP at 1 week **(S)** or 4 weeks **(T)** after SCI. Two-Way ANOVA with Tukey's multiple comparisons *post hoc* test. Uninjured groups were not included in the

analysis as their values were zeros. n=5 animals per uninjured group, n=6 for 1 week injured, n=7 for 4 weeks injured. Scale bar=500 μm for **(A–C)** and Scale bar=50 μm for **(J–L, P–R)** and Scale bar=10 μm for **(M–O)**.